Formation Mechanism of Anionic Surfactant-Templated Mesoporous Silica

Chuanbo Gao,[†] Huibin Qiu,[†] Wei Zeng,[†] Yasuhiro Sakamoto,*[,‡] Osamu Terasaki,[‡] Kazutami Sakamoto,[§] Qun Chen,[||] and Shunai Che*[,†]

School of Chemistry and Chemical Technology, State Key Laboratory of Composite Materials, Shanghai Jiao Tong University, Shanghai 200240, People's Republic of China, Structural Chemistry, Arrhenius Laboratory, Stockholm University, S-10691 Stockholm, Sweden, Research Center, Shiseido Company, Limited, 2-2-1, Hayabuchi, Tsuzuki-ku, Yokohama 224-8558, Japan, and Key Laboratory of Ministry of Education for Optical and Magnetic Resonance Spectroscopy, East China Normal University, Shanghai 200062, People's Republic of China

Received May 11, 2006. Revised Manuscript Received June 8, 2006

The synthesis mechanism of anionic surfactant-templated mesoporous silica (AMS) is described. A family of highly ordered mesoporous silica structures have been synthesized via an approach based on the self-assembly of anionic surfactants and inorganic precursors by using aminopropylsiloxane or quaternized aminopropylsiloxane as the co-structure-directing agent (CSDA), which is a different route from previous pathways. Mesophases with differing surface curvatures, varying from cage type (tetragonal $P4_2/mnm$; cubic $Pm\bar{3}n$ with modulations; cubic $Fd\bar{3}m$) to cylindrical (two-dimensional hexagonal $p6mm$), bicontinuous (cubic $Ia\bar{3}d$ and $Pn\bar{3}m$), and lamellar have been obtained by controlling the charge density of the micelle surfaces by varying the degree of ionization of the carboxylate surfactants. Changing the degree of ionization of the surfactant results in changes of the surfactant packing parameter g, which leads to different mesostructures. Furthermore, variation of the charge density of positively charged amino groups of the CSDA also gives rise to different values of g. Mesoporous silicas, functionalized with amino and quaternary ammonium groups and with the various structures given above, have been obtained by extraction of the surfactant. This report leads to a deeper understanding of the interactions between the surfactant anions and the CSDA and provides a feasible and facile approach to the mesophase design of AMS materials.

Introduction

Synthesis of mesoporous materials relies upon surfactant micelles as templates for the assembly and subsequent condensation of inorganic precursors.[1] It is common practice to divide surfactants into the classes of cationic, anionic, and nonionic. The well-ordered hexagonal, cubic, and lamellar mesoporous silicas (M41S family and SBA-1, -2, -3, -7, etc.) have been prepared by using cationic quaternary ammonium surfactants under both basic and acidic conditions, where the templating effect is based on electrostatic interactions.[2−7] Neutral nonionic surfactants (block copolymers) were used as templates to prepare mesoporous materials with large pores (HMS, SBA-11, -12, -15, -16 and FDU-1, -2, -5, etc.)[8−14] through hydrogen bonding or electrostatic interactions. However, only lamellar or disordered mesophases resulted from the use of anionic surfactants when silicate was the inorganic precursor, indicating that the structure-directing interaction between negatively charged headgroups of anionic surfactants and silicate species necessary to form ordered structures is difficult to achieve under acidic or basic conditions.

Recently, we have reported a new anionic surfactant templating route to mesoporous silica by introducing an additional structure-directing effect by inclusion of amino-

* To whom correspondence should be addressed. S.C.: fax, +86-21-5474-1297; tel., +86-21-5474-2852; e-mail, chesa@sjtu.edu.cn. Y.S.: e-mail, yasuhiro@struc.su.se.

[†] Shanghai Jiao Tong University.

[‡] Stockholm University.

[§] Shiseido Co.

[||] East China Normal University.

(1) Kresge, C. T.; Leonowicz, M. E.; Roth, W. J.; Vartuli, J. C.; Beck, J. S. *Nature* **1992**, *359*, 710−712.

(2) Beck, J. S.; Vartuli, J. C.; Roth, W. J.; Leonowicz, M. E.; Kresge, C. T.; Schmitt, K. D.; Chu, C. T.-W.; Olson, D. H.; Sheppard, E. W.; McCullen, S. B.; Higgins, J. B.; Schlenkert, J. L. *J. Am. Chem. Soc.* **1992**, *114*, 10834−11843.

(3) Huo, Q.; Margolese, D. I.; Ciesla, U.; Feng, P.; Gier, T. E.; Sieger, P.; Leon, R.; Petroff, P. M.; Schüth, F.; Stucky, G. D. *Nature* **1994**, *368*, 317−321.

(4) Huo, Q.; Margolese, D. I.; Ciesla, U.; Demuth, D. G.; Feng, P.; Gier, T. E.; Sieger, P.; Firouzi, A.; Chmelka, B. F.; Schüth, F.; Stucky, G. D. *Chem. Mater.* **1994**, *6*, 1176−1191.

(5) Huo, Q.; Margolese, D. I.; Stucky, G. D. *Chem. Mater.* **1996**, *8*, 1147−1160.

(6) Pantazis, C. C.; Pomonis, P. J. *Chem. Mater.* **2003**, *15*, 2299−2300.

(7) Huo, Q.; Leon, R.; Petroff, P. M.; Stucky, G. D. *Science* **1995**, *268*, 1324−1327.

(8) Tanev, P. T.; Pinnavaia, T. J. *Science* **1995**, *267*, 865−867.

(9) Bagshaw, S. A.; Prouzet, E.; Pinnavaia, T. J. *Science* **1995**, *269*, 1242−1244.

(10) Zhao, D.; Huo, Q.; Feng, J.; Chmelka, B. F.; Stucky, G. D. *J. Am. Chem. Soc.* **1998**, *120*, 6024−6036.

(11) Yu, C.; Tian, B.; Fan, J.; Stucky, G. D.; Zhao, D. *J. Am. Chem. Soc.* **2002**, *124*, 4556−4557.

(12) Zhao, D.; Feng, J.; Huo, Q.; Melosh, N.; Fredrickson, G. H.; Chmelka, B. F.; Stucky, G. D. *Science* **1998**, *279*, 548−552.

(13) Shen, S.; Li, Y.; Zhang, Z.; Fan, J.; Tu, B.; Zhou, W.; Zhao, D. *Chem. Commun.* **2002**, 2212−2213.

(14) Liu, X.; Tian, B.; Yu, C.; Gao, F.; Xie, S.; Tu, B.; Che, R.; Peng, L.-M.; Zhao, D. *Angew. Chem., Int. Ed.* **2002**, *41*, 3876−3878.

10.1021/cm061107+ CCC: $33.50
Published on Web 07/13/2006

propylsiloxane or quaternized aminopropylsiloxane in the inorganic precursors. These act as co-structure-directing agents (CSDAs); examples include 3-aminopropyltrimethoxysilane (APS) and *N*-trimethoxylsilylpropyl-*N*,*N*,*N*-trimethylammonium chloride (TMAPS).[15] The negatively charged headgroups of the anionic surfactants interact electrostatically with the positively charged ammonium sites of the CSDAs. The alkoxysilane groups of the CSDA co-condense with tetraalkoxysilane and are subsequently assembled to form the silica framework. The trimethylene groups of the APS and TMAPS covalently tether the silicon atoms to the cationic ammonium groups. Various mesophases, including tetragonal $P4_2/mnm$, three-dimensional hexagonal $P6_3/mmc$, cubic $Pm\bar{3}n$, cubic $Fd\bar{3}m$, two-dimensional hexagonal $p6mm$, bicontinuous cubic $Ia\bar{3}d$, bicontinuous cubic $Pn\bar{3}m$, a lamellar structure, a modulated structure, and a chiral mesostructure with helically arranged pores, were successfully prepared on the basis of this synthesis route with different surfactants and under various synthesis conditions.[15−20] This novel route, which proves successful in producing a diversity of structures, owes its unique characteristics to introduction of the CSDA. To the best of our knowledge, no report has systematically discussed the formation mechanism and mesophase control of anionic surfactant-templated mesoporous silica (AMS) materials.

In the synthesis of mesoporous materials, the energetics of self-organization has been thought of in two parts.[21] One part is the packing energetics of the surfactant,[5] and the other depends on charge density matching between the surfactant and the inorganic species.[22] The surfactant packing depends on the molecular geometry of the surfactants, such as the number of carbon atoms in the hydrophobic chain,[21] the degree of chain saturation,[23] the size or charge of the polar headgroup,[4,24] and the molecular shape.[25] In addition, it has been reported that the packing of the surfactant is also affected by the solution conditions, including the surfactant concentration,[26] the presence of cosurfactant[21] and counterion,[27,28] and temperature.[29] Monnier et al.[22] and Tolbert et al.[21] reported that the arrangement of cationic surfactant molecules can be affected by decreasing the negative charge density on the silicate wall during the mesophase formation, which results in a mesostructural change from lamellar to two-dimensional hexagonal. It was demonstrated that the surfactant packing is the dominant factor in determining the final structure of the mesoporous materials, and the matching between the interfacial charge density of the inorganic silica framework and the charge density of the surfactant headgroups affects the kinetics of the mesophase transition.[21,22]

Here we describe the formation mechanism of AMS family mesoporous materials through controlling the mesophases by a facile and effective method. Carboxylic acid surfactants, including fatty acids and amino acid surfactants, are common anionic surfactants and are widely used commodity chemicals. Unlike the quaternary ammonium cationic surfactants, carboxylic acid surfactants are weak acids, with a pK_a of about 1−5. Therefore, the equilibrium can usually be reached between the uncharged and the negatively charged surfactant molecules in solution. The degree of ionization of the surfactant (molar ratio of charged/total surfactant) can readily be changed in the presence of additional acid or base, which causes differences in the charge density of the micelles and results in different surfactant arrangements.[31] Our method is based on controlling the surfactant packing through changing the charge density of anionic micelles. The surfactant packing parameter g,[23] where $g = v/a_0 l$, has been used to describe the surfactant organization in the self-assembly arrays and to predict the resultant mesostructures, where v is the chain volume of the surfactant, a_0 is the effective hydrophobic/hydrophilic interfacial area, and l is the kinetic surfactant chain length. Small values of g usually favor more curved surfaces. The lower degree of ionization of surfactant contributes to the partial reduction in the electrostatic repulsion between the charged surfactant headgroups and a decrease in the effective headgroup area of surfactant, a_0, thus resulting in an increase in the g value (Scheme 1). Therefore, the mesophases can vary with the degree of ionization of the anionic surfactant, driven by the different arrangement of the surfactant and the state of the micelles.

The route differs from the cationic surfactant templating system in that the positive charges of the silica framework that are imparted by the CSDA remain during the mesophase formation, because the charged amino groups are covalently bonded to the silica wall. This charge density matching interaction between the headgroup of the surfactant and the silicate wall hinders mesophase transition. However, the positive charge density provided by CSDA does affect the surfactant arrays via their energetics. An increase in the positive charge density of the CSDA (APS) facilitates a

(15) Che, S.; Garcia-Bennett, A. E.; Yokoi, T.; Sakamoto, K.; Kunieda, H.; Terasaki, O.; Tatsumi, T. *Nat. Mater*. **2003**, *2*, 801−805.
(16) Garcia-Bennett, A. E.; Kupferschmidt, N.; Sakamoto, Y.; Che, S.; Terasaki, O. *Angew. Chem., Int. Ed*. **2005**, *44*, 5317−5322.
(17) Garcia-Bennett, A. E.; Miyasaka, K.; Terasaki, O.; Che, S. *Chem. Mater*. **2004**, *16*, 3597−3605.
(18) Garcia-Bennett, A. E.; Terasaki, O.; Che, S.; Tatsumi, T. *Chem. Mater*. **2004**, *16*, 813−821.
(19) Che, S.; Liu, Z.; Ohsuna, T.; Sakamoto, K.; Terasaki, O.; Tatsumi, T. *Nature* **2004**, *429*, 281−284.
(20) Gao, C.; Sakamoto, Y.; Sakamoto, K.; Terasaki, O.; Che, S. *Angew. Chem., Int. Ed*. **2006**, *45*, 4295−4298.
(21) Tolbert, S. H.; Landry, C. C.; Stucky, G. D.; Chmelka, B. F.; Norby, P.; Handon, J. C.; Monnier, A. *Chem. Mater*. **2001**, *13*, 2247−2256.
(22) Monnier, A.; Schüth, F.; Huo, Q.; Kumar, D.; Margolese, D.; Maxwell, R. S.; Stucky, G. D.; Krishnamurty, M.; Petroff, P.; Firouzi, A.; Janicke, M.; Chmelka, B. F. *Science* **1993**, *261*, 1299−1303.
(23) Israelachvili, J. N.; Mitchell, D. J.; Ninham, B. W. *J. Chem. Soc., Faraday Trans. 2* **1976**, *72*, 1525−1568.
(24) Kim, J. M.; Sakamoto, Y.; Hwang, Y. K.; Kwon, Y.-U.; Terasaki, O.; Park, S.-E.; Stucky, G. D. *J. Phys. Chem. B* **2002**, *106*, 2552−2558.
(25) Shen, S.; Garcia-Bennett, A. E.; Liu, Z.; Lu, Q.; Shi, Y.; Yan, Y.; Yu, C.; Liu, W.; Cai, Y.; Terasaki, O.; Zhao, D. *J. Am. Chem. Soc*. **2005**, *127*, 6780−6787.
(26) Vartuli, J. C.; Schmitt, K. D.; Kresge, C. T.; Roth, W. J.; Leonowicz, M. E.; McCullen, S. B.; Hellring, S. D.; Beck, J. S.; Schlenker, J. L.; Olson, D. H.; Sheppard, E. W. *Chem. Mater*. **1994**, *6*, 2317−2326.
(27) Che, S.; Lim, S.; Kaneda, M.; Yoshitake, H.; Terasaki, O.; Tatsumi, T. *J. Am. Chem. Soc*. **2002**, *124*, 13962−13963.
(28) Che, S.; Li, H.; Lim, S.; Sakamoto, Y.; Terasaki, O.; Tatsumi, T. *Chem. Matter*. **2005**, *17*, 4103−4113.
(29) Che, S.; Sakamoto, Y.; Terasaki, O.; Tatsumi, T. *Microporous Mesoporous Mater*. **2005**, *85*, 207−218.
(30) Carlsson, A.; Kaneda, M.; Sakamoto, Y.; Terasaki, O.; Ryoo, R.; Joo, S. H. *J. Electron Microsc*. **1999**, *48*, 795−798.
(31) Kaneko, D.; Plsson, U.; Sakamoto, K. *Langmuir* **2002**, *18*, 4699−4703.

Scheme 1. Electrostatic Interaction between the Anionic Surfactant and the CSDA[a]

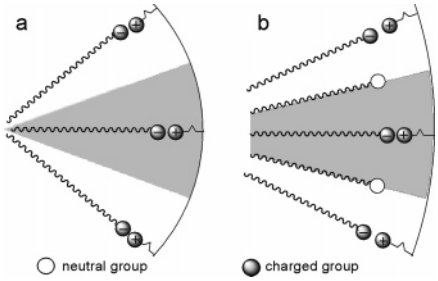

[a] The charge density on the micelles, characterized by the degree of ionization of the anionic surfactant, can vary, and results in different packing parameters *g*. a, smaller *g* created with higher degree of ionization; b, larger *g* created with lower degree of ionization.

decrease in the electrostatic repulsion between the anionic headgroups that in turn decreases the a_0 value and results in a larger *g* value. In summary, control of the packing parameter through ionization of the anionic surfactant makes the mesostructure of AMS materials more amenable to design and is the clearest advantage of AMS materials over other types of mesoporous materials. In a manner similar to the cationic surfactant templating route, formation of the mesostructure can be also affected by the geometry and concentration of surfactant and the molar ratios of silica source/surfactant and CSDA/surfactant. However, here we focus our discussion of the AMS synthesis mechanism on the role of the degree of ionization of the surfactant because it is so dramatic.

Experimental Section

Chemicals. APS (TCI), TMAPS (Azmax), tetraethyl orthosilicate (TEOS, TCI), and the sodium salt of myristic acid (C_{14}AS, TCI) were purchased and used as received. Anionic surfactants derived from amino acids (glutamic acid, alanine, valine, etc.) were synthesized.

Surfactant Preparation. In a typical synthesis of *N*-myristoyl-L-glutamic acid (C_{14}GluA), 120 mL of acetone, 19.2 g of sodium hydroxide, 49.3 g (0.2 mol) of myristoyl chloride, and 8.0 g (0.2 mol) of sodium hydroxide in 20 mL of water were added with stirring to a solution prepared from 35.5 g (0.24 mol) of L-glutamic acid in 140 mL of water, at 30 °C and pH 12 over a period of 20 min. The reaction mixture was stirred for 1 h additionally, cooled, and acidified to pH 1 with hydrochloric acid. The precipitated crystals of *N*-myristoyl-L-glutamic acid were purified by washing with petroleum ether.

The synthesis of alanine- and valine-derived surfactants, *N*-lauroyl-L-alanine (C_{12}AlaA) and *N*-palmitoryl-L-valine sodium salt (C_{16}ValS), is similar to the synthesis of C_{14}GluA. In the synthesis of C_{16}ValS the product was neutralized with an equivalent amount of NaOH in the final step.

Synthesis of Mesoporous Silica. In a typical synthesis of anionic surfactant-templated mesoporous silica AMS-9 (GluA-TM-NaOH-2.0 in the nomenclature of this paper), 0.357 g of C_{14}GluA was dissolved in deionized water at 80 °C. To the solution was added 2.0 g of 1 M NaOH with stirring. After the surfactant solution was cooled to 60 °C, a mixture of 3.12 g of TEOS and 0.773 g of TMAPS (50 wt % in methanol) was added with stirring. After 10 min the stirring was stopped, and the reaction mixture was aged at 60 °C for 2 days. The precipitate was filtered, dried at 60 °C, and calcined at 600 °C for 6 h to give surfactant-free mesoporous silica.

To obtain surfactant-free mesoporous silica functionalized with organic groups, the as-made samples were extracted by ethanolic solution of ethanolamine (17 vol %, for samples prepared with APS as CSDA) or of HCl (concentrated, 11 vol %, for samples prepared with TMAPS as CSDA) for 12−24 h at its boiling temperature.

Characterization. Powder X-ray diffraction (XRD) patterns were recorded on a Rigaku X-ray diffractometer D/MAX-2200/PC using Cu Kα radiation (40 kV, 20 mA) at the rate of 1.0° 2θ/min over the range of 1−6° 2θ. High-resolution transmission electron microscopy (HRTEM) was performed with a JEOL JEM-3010 microscope operating at 300 kV (C_s = 0.6 mm, resolution 1.7 Å). Images were recorded with a charge-coupled device camera (MultiScan model 794, Gatan, 1024 × 1024 pixels, pixel size 24 × 24 μm) at 50 000−80 000 K magnification under low-dose conditions. The nitrogen adsorption/desorption isotherms were measured at 77 K with a Quantachrome Nova 4200E porosimeter. The surface area was calculated by the Brunauer−Emmett−Teller (BET) method, and the pore size was obtained from the maxima of the pore size distribution curve calculated by the Barrett−Joyner−Halenda (BJH) method using the adsorption branch of the isotherm. Solid-state ^{13}C magic-angle spinning (MAS) NMR spectra of the mesoporous materials were collected on a Varian Mercury plus-400 NMR spectrometer. Thermogravimetric (TG) analyses of the materials were recorded on a Perkin-Elmer thermal gravimetric analyzer (TGA-7) from ambient temperature to 800 °C at the heating rate of 10 °C/min in all cases.

Results and Discussion

1. Mesophase Investigation of the TMAPS/Anionic Surfactant System. In the TMAPS/anionic surfactant system of the novel anionic surfactant templating route to mesoporous silica, the negatively charged headgroup of the anionic surfactants interacts with the positively charged ammonium site of TMAPS electrostatically, through the double decomposition of anionic surfactant salt and TMAPS quaternary ammonium salt.[15] The alkoxysilane sites of TMAPS are co-condensed with TEOS, to be assembled subsequently to form the silica framework. The trimethylene groups of TMAPS covalently tether the silicon atoms incorporated into the framework to the cationic ammonium groups. Figure 1 shows the XRD patterns of calcined mesoporous silica synthesized using C_{14}GluA as the template and TMAPS as the CSDA with addition of different amounts of NaOH. The samples are designated as GluA-TM-NaOH-*x*, where *x* denotes the molar ratio of NaOH/C_{14}GluA. Different mesophases have been obtained when *x* decreased from 2.4 to 0.75, which can be inferred from the different XRD patterns and HRTEM images (Figure 2).

The XRD patterns of the samples GluA-TM-NaOH-2.2 and -2.0 (Figure 1a,b) show main peaks at about 2.0−2.2° 2θ, and no detailed peaks can be observed; therefore, it is hard to index the peaks or further determine the space group from the XRD data. However, the HRTEM image of the sample GluA-TM-NaOH-2.0 taken along the [001] direction (Figure 2a) shows a large area of a uniform region, indicating that the mesophase is highly ordered. No three-fold axis can be observed, suggesting that the structure does not have cubic symmetry. On the basis of the tetragonal system it can be reasonably assigned to the $P4_2/mnm$ space group. Interestingly, the material shows good crystal morphology (Supporting Information, Figure S1), and fourfold axes can be

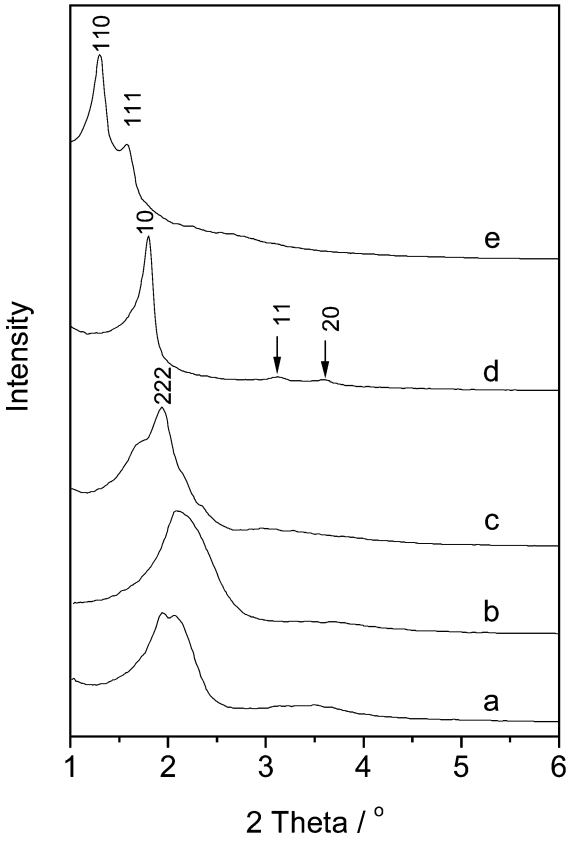

Figure 1. XRD patterns of calcined mesoporous silica synthesized by using C_{14}GluA as the template and TMAPS as the CSDA with addition of different amounts of base, NaOH. The compositions of the reaction mixtures are C_{14}GluA/TMAPS/TEOS/H_2O/NaOH = 1:1.5:15:2000:*x*, where *x* = (a) 2.2, (b) 2.0, (c) 1.5, (d) 1.0, and (e) 0.75. The precipitate was aged at 60 °C for 2 days. The samples are designated as GluA-TM-NaOH-*x*.

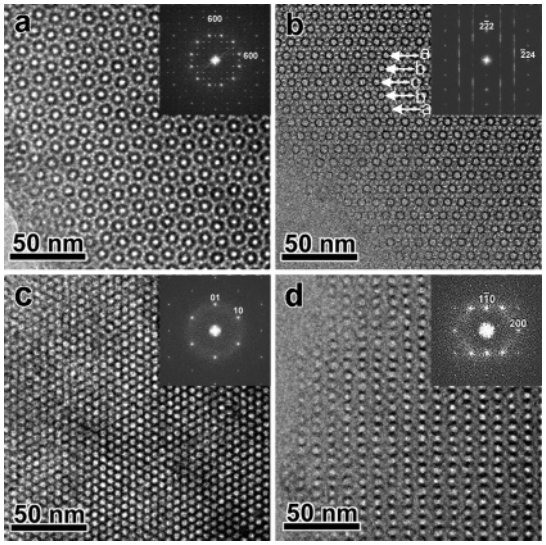

Figure 2. HRTEM images and Fourier diffractograms of the calcined mesoporous silica GluA-TM-NaOH-2.0 (a, [001]), GluA-TM-NaOH-1.5 (b, [110]), GluA-TM-NaOH-1.0 (c), and GluA-TM-NaOH-0.75 (d, [110]). The arrows indicate stacking faults of GluA-TM-NaOH-1.5 along the [111] direction.

easily observed consistent with the tetragonal space group. Considering the unit cell parameters calculated from HR-TEM, the space group shows many X-ray diffractions within 1−3° 2θ, making the XRD pattern difficult to resolve. This mesophase was obtained for the first time by using C_{12}GluA as the template and APS as the CSDA through a small delay

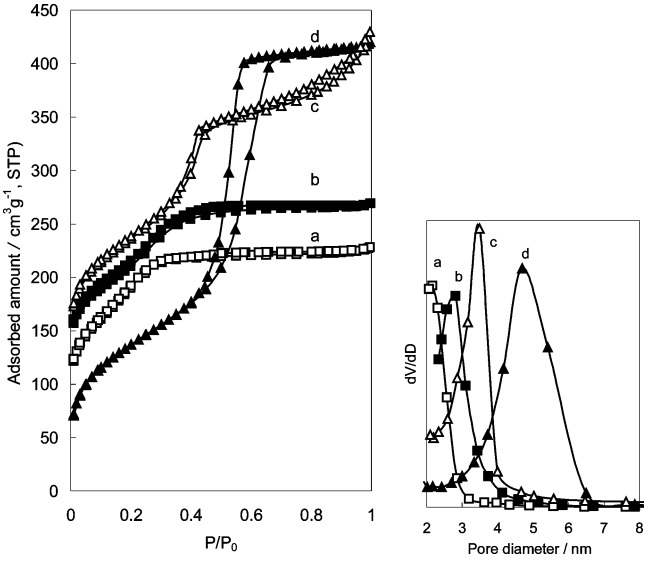

Figure 3. Nitrogen adsorption/desorption isotherms and pore size distributions (based on the adsorption branch and BJH method) of the calcined mesoporous silica GluA-TM-NaOH-2.0 (a), GluA-TM-NaOH-1.5 (b), GluA-TM-NaOH-1.0 (c), and GluA-TM-NaOH-0.75 (d). The isotherms a−c are offset vertically by 50, 100, and 100 cm^3/g STP, respectively.

in the time of addition of the silica source with respect to the CSDA and was named AMS-9.[16]

The XRD pattern of mesoporous silica GluA-TM-NaOH-1.5 (Figure 1c) is also difficult to index. However, the HRTEM image (Figure 2b) clearly indicates that the space group of the material is cubic $Fd\bar{3}m$ though there are a lot of stacking faults along the [111] direction, which give rise to diffuse scattering in the Fourier diffractogram. The main peak of the XRD pattern can be indexed as the (222) reflection based on the $Fd\bar{3}m$ symmetry, and the calculated unit cell parameter *a* is consistent with that calculated from HRTEM (a = 15.9 nm).

The sample GluA-TM-NaOH-1.0 obtained from a lower NaOH/C_{14}GluA molar ratio of 1.0 proves to be a typical two-dimensional hexagonal *p*6*mm* mesophase (Figure 1d). The three well-resolved peaks with a 1:$\sqrt{3}$:2 *d* spacing ratio can be indexed to (10), (11), and (20) reflections of a hexagonal structure with unit cell parameter a = 5.7 nm. The HRTEM image (Figure 2c) taken with the electron beam parallel to the channel axis shows well-ordered hexagonally arranged mesopores.

Figure 1e shows the XRD pattern of GluA-TM-NaOH-0.75 (AMS-10). The two well-resolved XRD peaks with a reciprocal spacings ($1/d_{hkl}$) ratio of $\sqrt{2}/\sqrt{3}$ can be indexed to (110) and (111) reflections, characteristic of the bicontinuous cubic $Pn\bar{3}m$ mesophase with unit cell parameter a = 9.6 nm, for the calcined sample. The HRTEM image taken along the [110] direction of the mesoporous material is shown in Figure 2d. The indices of the Fourier diffractogram are consistent with the extinction rules of the space group. Further electron crystallographic study shows that the mesostructure is composed of an enantiomeric pair of three-dimensional tetrahedrally connected mesoporous networks that are interwoven with each other.[20]

Figure 3 shows the nitrogen adsorption/desorption isotherms and pore size distribution curves of the mesoporous silica GluA-TM-NaOH-*x*. Details of the porosity of the

Table 1. Porous Properties of Mesoporous Silica Synthesized with C_{14}GluA and TMAPS, GluA-TM-NaOH-*x*

sample	mesostructure (space group)	pore type	surface area ($m^2\ g^{-1}$)	pore volume ($cm^3\ g^{-1}$)	pore diameter (nm)
GluA-TM-NaOH-2.0	tetragonal ($P4_2/mnm$)	cage type	535	0.276	2.2
GluA-TM-NaOH-1.5	cubic ($Fd\bar{3}m$)	cage type	421	0.262	2.8
GluA-TM-NaOH-1.0	two-dimensional hexagonal ($p6mm$)	cylindrical	495	0.510	3.5
GluA-TM-NaOH-0.75	cubic ($Pn\bar{3}m$)	cylindrical	493	0.650	4.7

samples are summarized in Table 1. All the samples show type IV isotherms, typical for mesoporous materials, and three well-distinguished regions of the adsorption isotherm are noticed including monolayer−multilayer adsorption, capillary condensation, and multilayer adsorption on the outer surface. No defined hysteresis loop is observed in the adsorption and desorption cycle around the capillary condensation on GluA-TM-NaOH-*x*, where $x = 2.0$, 1.5, or 1.0, due to the small size of the mesopores. However, for sample GluA-TM-NaOH-0.75 synthesized in the presence of less NaOH, a clear hysteresis loop of H1 type is observed and the capillary condensation occurs at a high relative pressure, indicating large cylindrical mesopores. Interestingly, the pore size distribution curves, BJH plots of derivative of the pore volume per unit weight with respect to the pore diameter (d*V*/d*D*) versus the pore diameter (*D*), show a clear shift of pore diameter from 2.2 to 4.7 nm as the molar ratio of NaOH/C_{14}GluA changes from 2 to 0.75.

When the molar ratio of NaOH/C_{14}GluA is decreased, the resultant mesophases change from tetragonal $P4_2/mnm$ and cubic $Fd\bar{3}m$ to two-dimensional hexagonal $p6mm$ and bicontinuous cubic$Pn\bar{3}m$. Tetragonal $P4_2/mnm$ and cubic $Fd\bar{3}m$ are both cage type mesophases, showing the largest surface curvatures ($g < 1/3$), while $p6mm$ ($g = 1/2$) and $Pn\bar{3}m$ ($g > 1/2$) are cylindrical, showing lower surface curvatures with larger g values. This sequence of mesophases can be explained by the different surfactant packing which is dependent on the degree of ionization of the surfactant. A reduced NaOH/C_{14}GluA molar ratio gives a lower degree of ionization of the anionic surfactant and thus a lower negative charge density of the micelles, which contributes to the reduction of the electrostatic repulsion between the surfactant headgroups and facilitates a reduced effective headgroup area a_0 and a larger g value. It supports the dominant role of the surfactant packing in the mesophase formation of AMS.

In a manner similar to that of the GluA-TM-NaOH-*x* system described above, changes in the resultant mesophases have also been observed when the one-headed carboxylate surfactants were partially neutralized by acid. XRD patterns of the mesoporous silica synthesized using C_{16}ValS as the template and introducing different amounts of HCl into the reaction system are shown in Figure 4. The samples are designated as ValS-TM-HCl-*x*, where *x* denotes the molar ratio of HCl/C_{16}ValS.

The XRD pattern of ValS-TM-HCl-0.1 shows two well-resolved peaks within 1−6° 2θ, corresponding to diffractions 1 and 2 of a layered structure. After calcination no peaks remained, indicating that the mesophase is unstable to surfactant removal.

ValS-TM-HCl-0.05 shows the XRD pattern of the bicontinuous cubic $Ia\bar{3}d$ mesophase. The reciprocal spacings ratio

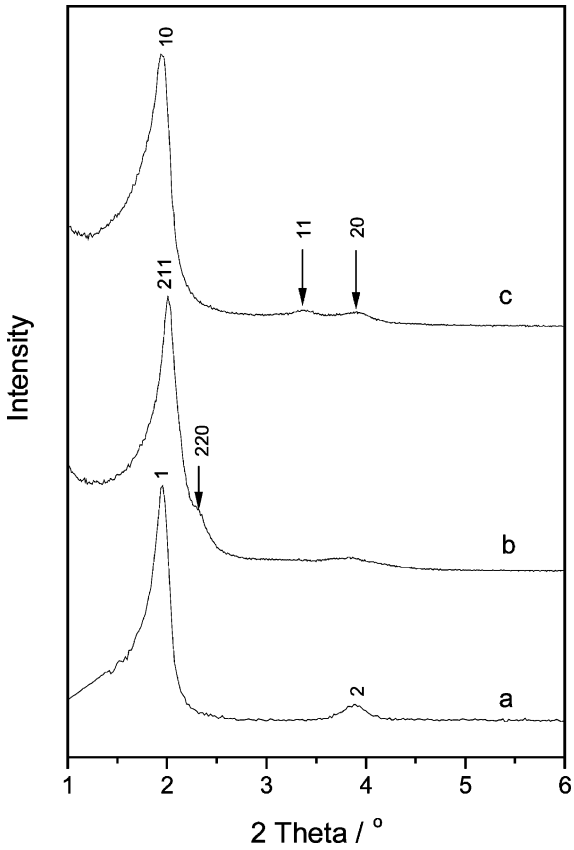

Figure 4. XRD patterns of mesoporous silica synthesized with C_{16}ValS. The compositions of the reaction mixtures are C_{16}ValS/TMAPS/TEOS/H_2O/HCl = 1:0.5:7:1978:*x*, where $x = 0.1$ (a, as-made), 0.05 (b, calcined), and 0 (c, calcined). The precipitate was aged at 60 °C for 2 days. The samples are designated as ValS-TM-HCl-*x*.

of the first two peaks is close to $\sqrt{3}/2$, in agreement with there being the (211) and (220) reflections. The HRTEM image taken along [311] direction (Figure 6a) confirms the space group. This mesophase has been extensively studied because it is common in liquid crystal systems and cationic and nonionic surfactant-templated mesoporous silica. In a similar way to the $Ia\bar{3}d$ phase, this structure comprises of a racemic pair of triangularly connected chiral networks.[30]

If no additional acid is added into the synthesis system, the XRD pattern of ValS-TM-HCl-0 shows three peaks within 1−4° of 2θ with reciprocal spacing ratios of about 1:$\sqrt{3}$:2, well-indexed on a two-dimensional hexagonal lattice.

The change in the mesophase of the products from lamellar to two-dimensional hexagonal $p6mm$ through bicontinuous cubic $Ia\bar{3}d$ with increasing surface curvatures occurs as a result of the decreasing amount of acid added into the reaction mixture using one-headed carboxylate surfactant as the template and TMAPS as the CSDA. It can be attributed to the increase in the degree of ionization of the surfactant and a decrease in the g value due to the increased effective headgroup area a_0 as discussed above. Furthermore, com-

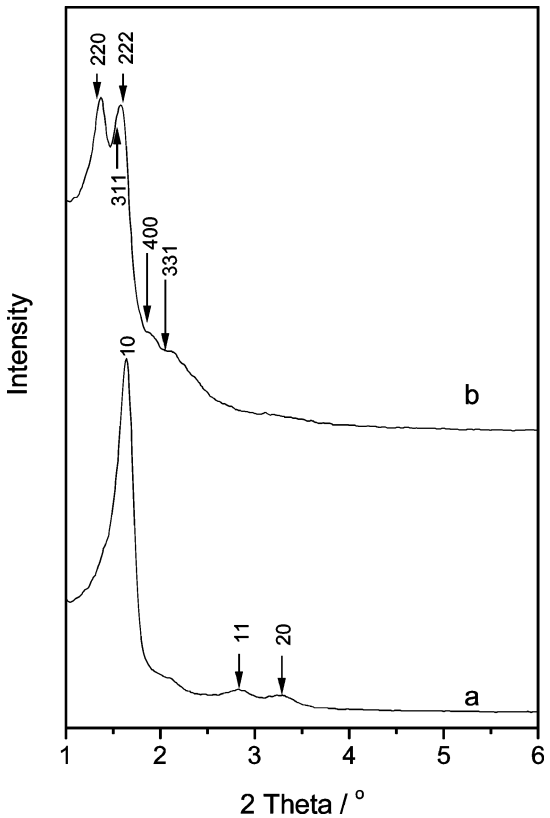

Figure 5. XRD patterns of calcined mesoporous silica synthesized with C_{14}AS. The compositions of the reaction mixtures are C_{14}AS/TMAPS/TEOS/H_2O/NaOH = 1:1:7:1389:*x*, where *x* = (a) 0 and (b) 0.1. The precipitate was aged at 60 °C for 2 days. The samples are designated as C14S-TM-NaOH-*x*.

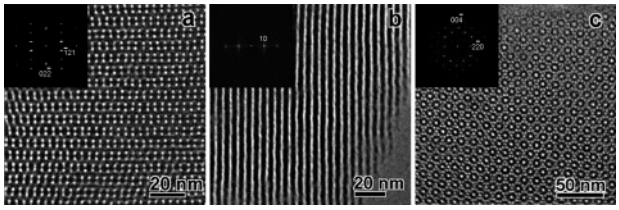

Figure 6. HRTEM images and Fourier diffractograms of calcined mesoporous silica ValS-TM-HCl-0.05 (a, [311]), C14S-TM-NaOH-0 (b), and C14S-TM-NaOH-0.1 (c, [110]).

parison of the gel compositions indicates that the amount of acid required to direct the synthesis of different mesophase products is small, which suggests that the mesostructure is sensitive to the acidity of the reaction solution and the change in the mesophase that crystallizes is caused by changing the degree of ionization of the surfactant.

When adding base (NaOH, for example) into the similar reaction system, the degree of ionization of surfactant will get larger, because higher pH facilitates ionization of the surfactant according to the chemical equilibrium. Therefore, mesophases with larger surface curvatures will be obtained. Figure 5 shows the XRD patterns of calcined mesoporous silica synthesized with C_{14}AS as the template and TMAPS as the CSDA, with or without addition of NaOH. The samples are designated as C14S-TM-NaOH-*x*, where *x* denotes the molar ratio of NaOH/C_{14}AS.

The sample C14S-TM-NaOH-0 obtained without addition of NaOH has a two-dimensional hexagonal mesostructure, as seen by the XRD pattern (Figure 5a) and the HRTEM

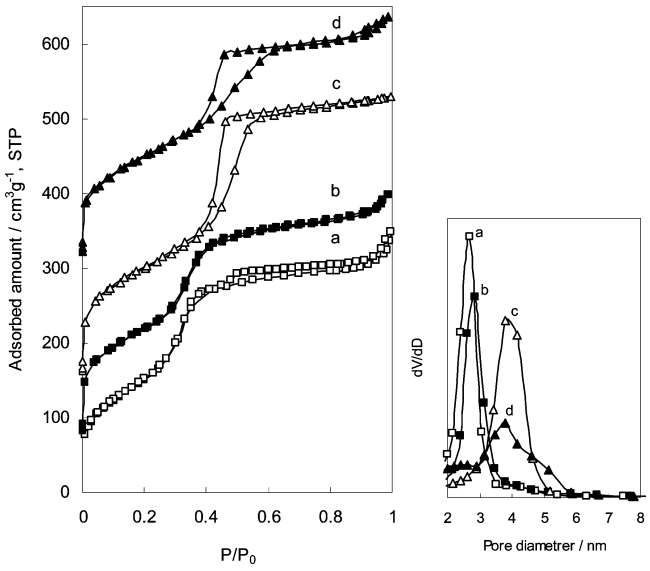

Figure 7. Nitrogen adsorption/desorption isotherms and pore size distributions (based on the adsorption branch and BJH method) of the calcined mesoporous silica ValS-TM-HCl-0.05 (a), ValS-TM-HCl-0 (b), C14S-TM-NaOH-0 (c), and C14S-TM-NaOH-0.1 (d). The isotherms b−d are offset vertically by 80, 160, and 320 cm^3/g STP, respectively.

image taken with the electron beam perpendicular to the hexagonally arranged mesopores (Figure 6b). Adding a small amount of NaOH to the reaction system (C14S-TM-NaOH-0.1) gives the cage type $Fd\bar{3}m$ mesophase structure with a smaller *g* value as expected, as determined from the XRD pattern (Figure 5b) and the HRTEM image taken along [110] direction (Figure 6c). Different from GluA-TM-NaOH-1.5, this mesophase is highly ordered with almost no stacking faults and gives a Fourier diffractogram with good quality. The XRD pattern can be indexed as shown in Figure 5b, and the unit cell *a* calculated from XRD data is consistent with that calculated from HRTEM (a = 19.1 nm).

The nitrogen adsorption/desorption isotherms and pore size distributions of the samples ValS-TM-HCl-*x* and C14S-TM-NaOH-*x* are shown in Figure 7, and the adsorption properties are summarized in Table 2. All the isotherms are typical reversible type IV adsorption isotherms as defined by IUPAC. The hysteresis loops in the adsorption and desorption cycles on the capillary condensation step of ValS-TM-HCl-*x* are not obvious because of the small pore sizes. The isotherm C14S-TM-NaOH-0 shows a typical H1 hysteresis loop within the relative pressure range of p/p_0 = 0.35−0.6, suggesting a cylindrical pore system, compared with that of C14-TM-NaOH-0.1, which shows a typical H2 hysteresis loop indicating a cage type mesophase, consistent with the HRTEM observations.

A general trend is observed in the type of mesophase prepared when using anionic surfactant as the template and TMAPS as the CSDA, changing from cage type (tetragonal $P4_2/mnm$ and cubic $Fd\bar{3}m$) to cylindrical (two-dimensional hexagonal $p6mm$, bicontinuous cubic $Ia\bar{3}d$, and bicontinuous cubic $Pn\bar{3}m$) and lamellar phase, upon changing the acidity or alkalinity of the reaction system. The degree of ionization of the surfactant is strongly affected by the pH of the synthesis system: A higher degree of ionization of the surfactant gives rise to stronger electrostatic repulsion between surfactant headgroups, a larger effective headgroup

Table 2. Porous Properties of Mesoporous Silica Synthesized with C_{16}ValS/C_{14}AS and TMAPS, ValS-TM-HCl-*x* and C14S-TM-NaOH-*x*

sample	mesostructure (space group)	pore type	surface area ($m^2\ g^{-1}$)	pore volume ($cm^3\ g^{-1}$)	pore diameter (nm)
ValS-TM-HCl-0.1	lamellar	layered			
ValS-TM-HCl-0.05	cubic (*Ia*$\bar{3}$*d*)	cylindrical	566	0.54	2.7
ValS-TM-HCl-0	two-dimensional hexagonal (*p6mm*)	cylindrical	533	0.49	2.8
C14S-TM-NaOH-0	two-dimensional hexagonal (*p6mm*)	cylindrical	511	0.57	3.8
C14S-TM-NaOH-0.1	cubic (*Fd*$\bar{3}$*m*)	cage type	385	0.49	3.8

area a_0, and a lower g value. The exact structure type of mesophase products is determined also by the molecular structure of the surfactants used. It is worth noting that the mesophase is formed with the aid of the CSDA, which provides the positive charge required for charge density matching with surfactant anions. The properties and concentrations of CSDA also determine the final mesostructure. In this study, the types and molar compositions of the CSDA and silica source were kept the same to enable the synthesis systems to be compared. It is also worth pointing out that, in these synthesis systems, where pH is in the range of 6−9, the silicate species show partial negative charges (isoelectric point p$I \approx 2$), but compared to the quaternary ammonium groups co-condensed with the silicate species the effect of any change in the negative charge density of the silicate with pH in this anionic surfactant templating pathway is likely to be insignificant. Therefore, it is reasonable to interpret the observed changes in the structure of the mesophases formed in terms of the degree of ionization of the surfactant, which is very sensitive to the acidity or alkalinity of the synthesis system.

2. Mesophase Investigation of the APS/Anionic Surfactant System. Besides TMAPS, APS is also an effective CSDA, and a variety of mesostructures involving its use have already been reported.[15−19] The negatively charged headgroups of the anionic surfactants interact electrostatically with the positively charged ammonium site of APS, through the neutralization of the various acids (p$K_a = 1-5$) and APS (p$K_b \approx 3.4$).[15] APS possesses basic character and can be protonated and charged in combination with acid, which is different from TMAPS.

Figure 8 shows the XRD patterns of calcined mesoporous silica synthesized with C_{14}GluA as the template and APS as the CSDA, and different amounts of acid were added into the reaction system. The molar compositions of the reaction mixtures are C_{14}GluA/APS/TEOS/H_2O/HCl = 1:4:15:2000:*x*, where *x* varies from 0 to 3.0, and the samples are designated as GluA-AP-HCl-*x*. A change in mesophase product can be achieved, as shown by the different XRD patterns.

The HRTEM image of the sample GluA-AP-HCl-0 is shown in Figure 9a, and a modulated cage type mesophase can be observed. The mesophase shows *Pm*$\bar{3}$*n* type contrast, but there is no long-range ordering. This type of mesophase has been designated AMS-2, which was first synthesized from a similar system by using C_{12}GluA as the template. Figure 9b shows the HRTEM image of the sample GluA-AP-HCl-1.6 taken along the [110] direction, from which the space group of the sample can be determined as *Fd*$\bar{3}$*m*. The mesostructure, together with GluA-AP-HCl-0, is cage type, showing a high surface curvature.

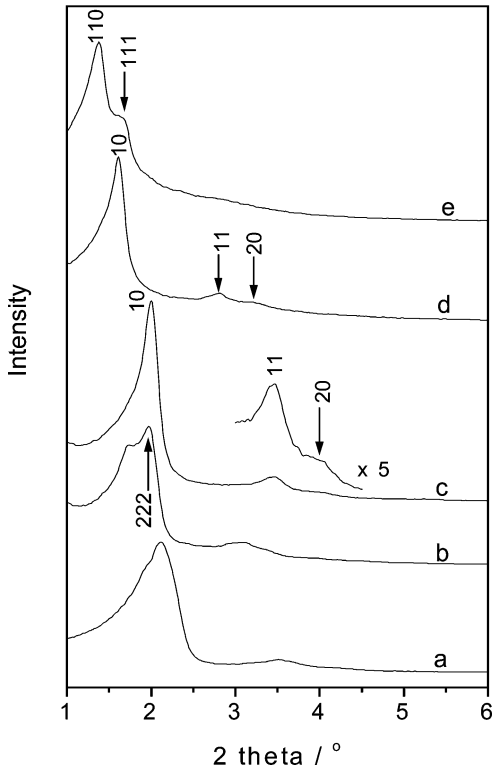

Figure 8. XRD patterns of calcined mesoporous silica synthesized by using C_{14}GluA as the template and APS as the CSDA with addition of different amounts of acid. The compositions of reaction mixtures are C_{14}GluA/APS/TEOS/H_2O/HCl = 1:4:15:2000:*x*, where *x* = (a) 0, (b) 1.6, (c) 2.4, (d) 2.8, and (e) 3.0. The precipitate was aged at 80 °C for 2 days. The samples are designated as GluA-AP-HCl-*x*.

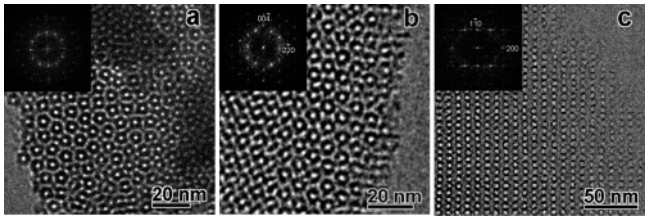

Figure 9. HRTEM images and Fourier diffractograms of calcined mesoporous silica GluA-AP-HCl-0 (a), GluA-AP-HCl-1.6 (b, [110]), and GluA-AP-HCl-3.0 (c, [110]).

The XRD patterns of mesoporous silica GluA-AP-HCl-2.4 and -2.8 (Figure 8c,d) exhibit three peaks that can be indexed on the basis of the two-dimensional hexagonal *p6mm* plane group. The HRTEM images (not shown) confirm the mesostructure. It is interesting that the two mesophases with the same symmetry were prepared with the same surfactant and under similar conditions, but the unit cells are of different sizes, which may indicate different curvatures of the cylindrical porous structures, as a result of different amounts of acid introduced into the reaction system. It is worth noting that the unit cell parameters *a* of the mesophases change continuously (not shown) from 5.1 to 6.3 nm when the amount of acid added into the synthesis system increases

Table 3. Porous Properties of Mesoporous Silica Synthesized with C_{14}GluA and APS, GluA-AP-HCl-*x*

sample	mesostructure (space group)	pore type	surface area ($m^2\ g^{-1}$)	pore volume ($cm^3\ g^{-1}$)	pore diameter (nm)
GluA-AP-HCl-0	modulated mesophase	cage type	540	0.30	2.4
GluA-AP-HCl-1.6	cubic ($Fd\bar{3}m$)	cage type	616	0.48	2.9
GluA-AP-HCl-2.4	two-dimensional hexagonal ($p6mm$)	cylindrical	813	0.68	3.1
GluA-AP-HCl-2.8	two-dimensional hexagonal ($p6mm$)	cylindrical	805	0.89	3.9
GluA-AP-HCl-3.0	cubic ($Pn\bar{3}m$)	cylindrical	673	0.81	4.2

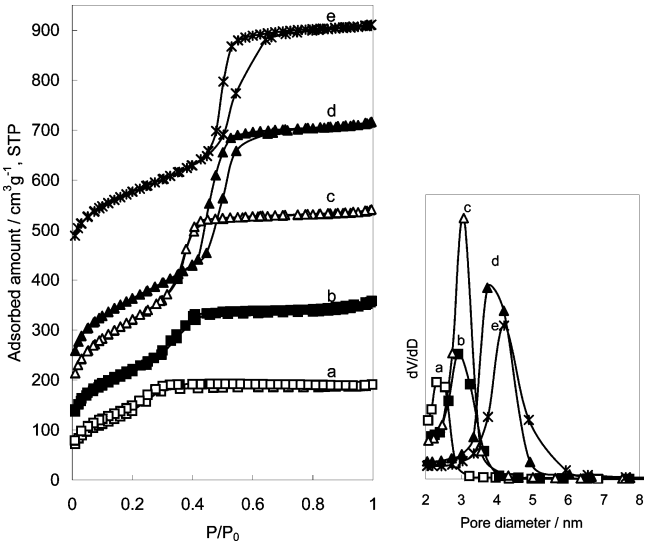

Figure 10. Nitrogen adsorption/desorption isotherms and pore size distributions (based on the adsorption branch and BJH method) of the calcined mesoporous silica (a) GluA-AP-HCl-0, (b) GluA-AP-HCl-1.6, (c) GluA-AP-HCl-2.4, (d) GluA-AP-HCl-2.8, and (e) GluA-AP-HCl-3.0. The isotherms b−e are offset vertically by 50, 100, 140, and 370 cm^3/g STP, respectively.

from 2.4 to 2.8, together with the change of the pore size (Table 3) from 3.1 to 3.9 nm.

Sample GluA-AP-HCl-3.0 shows an XRD pattern (Figure 8e) similar to that of GluA-TM-NaOH-0.75. Two peaks can be distinguished with a reciprocal spacings ratio of about $\sqrt{2}/\sqrt{3}$, and the HRTEM image taken along the [110] direction (Figure 9c) clearly shows that the space group of the mesoporous material is bicontinuous cubic $Pn\bar{3}m$. It can be inferred that the $Pn\bar{3}m$ space group structure is a readily obtained mesophase independent of the type and also the amount of CSDA, but it may be that it is strongly controlled by the structure of the surfactant, because in our experiments only two-headed anionic surfactants have templated this mesophase.

The nitrogen adsorption/desorption isotherms of the mesoporous materials GluA-AP-HCl-*x* are shown in Figure 10, and the porous properties are shown in Table 3. All the samples show typical type IV isotherms. It can be seen from the pore size distribution curves that the pore diameters shift gradually from 2.4 to 4.2 nm as the product changes from cage type to cylindrical, with higher amounts of acid added. Accordingly, capillary condensation is observed at a higher pressure, and the hysteresis loops become more evident.

The mesostructure that results using anionic surfactants as templates and APS as the CSDA is, therefore, strongly dependent on the amount of acid introduced into the reaction system. The product changes from cage type mesophases (the modulated cage type mesophase AMS-2 and the cubic $Fd\bar{3}m$ phase) to those containing channels of uniform

Scheme 2. Illustration of the Mesophase Formation when Anionic Surfactant Is Used as the Template and APS Is Used as the CSDA[a]

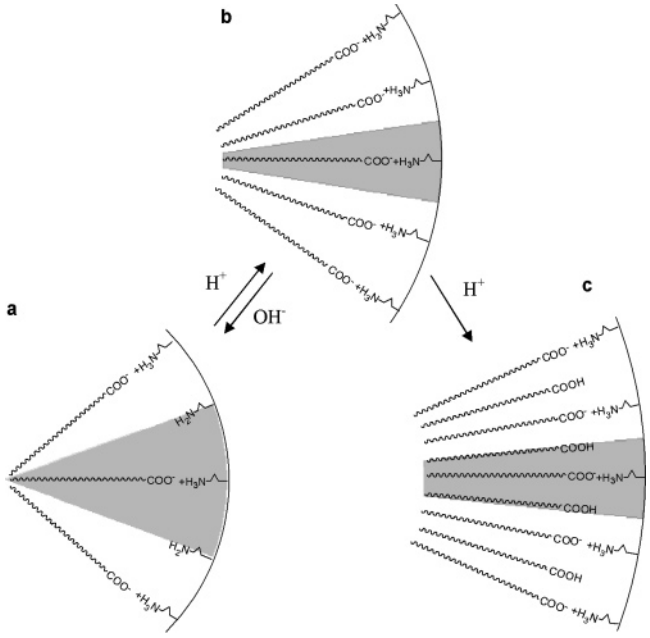

[a] (a) With excess of base (including NaOH and APS), (b) without excess of base or acid, and (c) with excess of acid (including HCl and carboxyl acid surfactant).

diameter (two-dimensional hexagonal $p6mm$ and bicontinuous cubic $Pn3m$) with structures with lower curvatures being formed as more acid is added.

Generally, the pK_b of carboxylate surfactants is about 9−13, and the pK_b of APS is nearly 3.4; therefore, APS is protonated by both HCl and carboxylic acid surfactant. The effect of the HCl can be considered in two compositional regions: when HCl/−COOH < 1 and > 1. In the glutamic acid surfactant synthesis system, the starting APS/−COOH molar ratio is 2. If HCl/−COOH < 1 (GluA-AP-HCl-0 and GluA-AP-HCl-1.6 in which HCl/−COOH = 0.8), APS will be protonated by both HCl and carboxylic acid, and the surfactant molecules are almost all charged. With the addition of different amounts of HCl in this range, the degree of protonation of APS will be changed and impart different charge densities to the inorganic oligomers. The presence of opposite charges next to the surfactant headgroups is expected to decrease the repulsion that results in a decrease in the a_0 value and an increase in the g value.[27,28] The positive charges of the inorganic species may also affect the arrangement of the mesocages. As a result, change in the product mesophase from a modulated cage type structure to a material with cubic $Fd\bar{3}m$ symmetry is achieved by increasing the amount of acid in the system (Scheme 2a to b). Cage type mesophases have been synthesized over a relatively wide range of HCl/surfactant molar ratios, and the phase selectivity

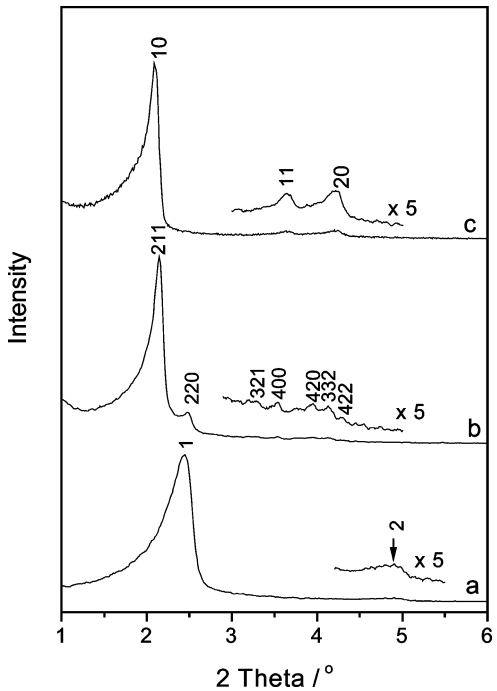

Figure 11. XRD patterns of mesoporous silica synthesized by using C_{12}-AlaA as the template and APS as the CSDA with addition of different amounts of base. The compositions of the reaction mixtures are C_{12}AlaA/APS/TEOS/H_2O/NaOH = 1:1:7:1500:*x*, where *x* = (a) 0, as-made, (b) 0.2, as-made, and (c) 0.8, calcined. The precipitate was aged at 60 °C for 2 days. The samples are designated as AlaA-AP-NaOH-*x*.

is insensitive to the amount of HCl, because of the indirect effect of acid on the surfactant packing.

When more acid (the starting HCl/−COOH > 1) was used in the synthesis system (GluA-AP-HCl-2.4, GluA-AP-HCl-2.8, and GluA-AP-HCl-3.0, in which HCl/−COOH = 1.2, 1.4, and 1.5, respectively), the carboxylate groups of the surfactant will be partially protonated, resulting in a significant decrease in the electrostatic repulsions between surfactant headgroups and, therefore, an increase in the *g* value. As a result, the stable mesophases are two-dimensional hexagonal and bicontinuous cubic with low curvatures. (Scheme 2b to c). This change in phase selectivity, triggered by the direct effect of the solution acidity on the surfactant arrangement, is very sensitive and gives rise to many different structure types.

The mesophase formation in the APS/surfactant system is related to the nature of the surfactant in a similar way to that described previously using TMAPS as the CSDA. When using one-headed anionic surfactant as the template, for example, C_{12}AlaA, a different sequence of phase selectivity can be observed from the XRD patterns shown in Figure 11. The gel compositions are C_{12}AlaA/APS/TEOS/H_2O/NaOH = 1:1:7:1500:*x*, where *x* = 0−1.0. The samples are designated as AlaA-AP-NaOH-*x*.

The mesophases can be easily identified from the XRD patterns. AlaA-AP-NaOH-0 is a typical lamellar phase (the XRD peaks can be indexed as reflections 1 and 2) whereas AlaA-AP-NaOH-0.2 is a bicontinuous cubic $Ia\bar{3}d$ mesophase (the reciprocal spacings ratio of the first two peaks is close to $\sqrt{2}/\sqrt{3}$, and thus the peaks can be indexed as (211) and (220) reflections. Even the minor peaks within 3−4.5° 2θ can be indexed, indicating the high quality of the mesophase).

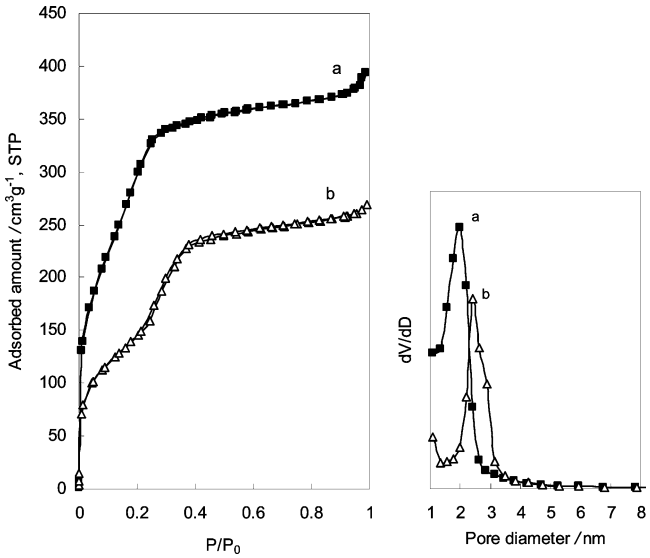

Figure 12. Nitrogen adsorption/desorption isotherms and pore size distributions (based on the adsorption branch and BJH method) of the calcined mesoporous silica (a) AlaA-AP-NaOH-0.2 and (b) AlaA-AP-NaOH-0.8.

AlaA-AP-NaOH-0.8 is two-dimensional hexagonal (from the (10), (11), and (20) reflections with a *d* spacing ratio of 1:1/$\sqrt{3}$:1/2).

The nitrogen adsorption/desorption isotherms of the samples AlaA-AP-NaOH-*x* are shown in Figure 12, and their adsorption properties are summarized in Table 4. It can be seen that the pore sizes of the materials are very small (2.0−2.4 nm calculated by the BJH method) because of the short chains of the surfactant. In this reaction system, using one-headed anionic surfactant as the template and APS as the CSDA, the mesophases with higher surfactant packing parameter *g* tend to be formed due to the small headgroup areas. By introducing some base, nonlamellar phases such as $Ia\bar{3}d$ and *p*6*mm* can be obtained. This may be attributed to lowering of the positive charge density on the inorganic species as the degree of protonation of APS is decreased by the additional base, which makes it unable to maintain the compact surfactant arrangement as the headgroups move apart from each other due to increased electrostatic repulsion. This gives a mesophase with a slightly higher curvature (Scheme 2b to a). The change in mesophase formation achieved by changing the positive charge density on the inorganic species is also based on an indirect effect of alkalinity on the surfactant packing, and the compositional fields are very large as a result.

3. Mesoporous Silica Functionalized with Amino or Quaternary Ammonium Groups. To obtain mesoporous silica functionalized with amino or quaternary ammonium groups, the as-made samples were extracted by ethanol solution with ethanolamine for samples prepared with APS as the CSDA or with HCl for samples prepared with TMAPS as the CSDA, respectively. All of the extracted samples show well-resolved XRD patterns similar to those of the calcined samples with various mesostructures confirmed by HRTEM analysis (not shown). The functional groups were confirmed by the solid-state ^{13}C MAS NMR spectra of the mesoporous materials after extraction (Figure 13). The strong resonance peaks, assignable to CH_2 (25−30 ppm) of the surfactants,

Table 4. Porous Properties of Mesoporous Silica Synthesized with C_{12}AlaA and APS, AlaA-AP-NaOH-*x*

sample	mesostructure (space group)	pore type	surface area ($m^2\ g^{-1}$)	pore volume ($cm^3\ g^{-1}$)	pore diameter (nm)
AlaA-AP-NaOH-0	lamellar	layered			
AlaA-AP-NaOH-0.2	cubic ($Ia\bar{3}d$)	cylindrical	1164	0.61	2.0
AlaA-AP-NaOH-0.8	two-dimensional hexagonal ($p6mm$)	cylindrical	643	0.42	2.4

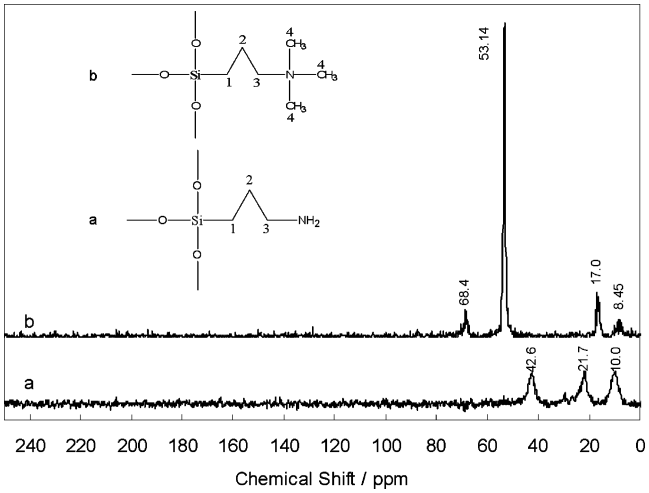

Figure 13. Solid-state ^{13}C MAS NMR spectra of the mesoporous materials after extraction: (a) materials synthesized with APS and extracted with ethanolamine/ethanol; (b) materials synthesized with TMAPS and extracted with HCl/ethanol.

disappeared after extraction, indicating that the surfactants were completely extracted. No resonance signal was detected around 180 ppm, where the signal from the −COOH group is expected. NMR of the extracted mesoporous silica synthesized with APS as the CSDA shows three resonance signals at 10.0, 21.7, and 42.6 ppm that could be assigned to C_1, C_2, and C_3 of APS, respectively. The resonance signals of the mesoporous silica synthesized with TMAPS as the CSDA at 8.45, 17.0, 53.14, and 68.4 ppm can be assigned to C_2, C_1, C_4, and C_3 of TMAPS, respectively. These demonstrate that the surfactant molecules were removed and amino and quaternary amine groups are present on the surface of mesopores. Elemental analysis results showed that carbon contained in the material is attributed to the hydrolysis and co-condensation of the CSDA. Almost all of the APS and TMAPS introduced to the synthesis system were co-condensed and are present on the pore surface of the mesoporous silica.

4. Discussion. As can be concluded from the experimental results, if all the other conditions were kept constant (i.e., the surfactant concentration, the amount of the CSDA and TEOS, the reaction temperature, and the aging time), the addition of acid or base into the reaction system has a very marked effect on the resultant mesophases, even for low added amounts. The pH of the reaction gel is typically 6−9, and this change of the gel pH is able to change the mesophase product from cage type with a high surface curvature to bicontinuous cubic and lamellar with lower surface curvatures. For example, the reaction gel containing C_{14}AS, TMAPS, TEOS, and H_2O (initial pH = 8.73) results in a mesophase of two-dimensional hexagonal $p6mm$ at 80 °C, while the gel containing 4 mM of NaOH (initial pH = 8.85) gives rise to a mesophase of cubic $Fd\bar{3}m$, which shows a higher surface curvature (Figure 5). This is different from what is observed for cationic or nonionic surfactant-templated mesoporous silica, because in those cases the final mesophase is relatively insensitive to small changes of the solution pH. The contribution of the pH difference in such a small range to the rate of condensation of the silica source can be neglected. The sensitivity of the mesophases formed to the acidity or alkalinity of the reaction system observed in our studies has been attributed to the variable charge of anionic surfactant micelles. Kaneko et al. and Acharya et al. reported that in the aqueous anionic surfactant solutions containing acylglutamate[31] or acylalaninate[32] the liquid crystalline phases change from lamellar to cubic and further to hexagonal when the degree of ionization of the surfactant gets larger, which is consistent with our experimental observations in mesoporous silica and supports our explanation of the mesophase transformation responding to the acidity or alkalinity of the reaction system.

Therefore, it can be concluded that the formation of the mesophase has been dominated by the surfactant packing. The key factor is the degree of ionization of the surfactant. Because many anionic surfactants are carboxylic acids (weak acids), the ionization of the surfactant can readily be controlled by changing the acidity or alkalinity of the synthesis system. It is an outstanding characteristic of the AMS family of mesoporous silicas that the mesophase product may be changed simply by controlling the initial acidity or alkalinity of the reaction solution. The arrangement of surfactant molecules into micelles can also be affected by the positive charge density of the inorganic species, and this can also be exploited to control the mesostructure, though this effect is not as direct as controlling the degree of ionization of the surfactant.

We have explained the change in mesophase product selectivity from cage type to cylindrical channel and lamellar that is triggered by changes in the acidity or alkalinity of the synthesis system in terms of the g parameter. However, it is difficult to explain the different mesophase selectivities within the same type of mesophase, for example, among the cage type $P4_2/mnm$, $Fd\bar{3}m$, and modulated structures, by the same reasoning. Nevertheless, these mesophases are also controlled by the acidity or alkalinity of the reaction solution, as indicated by our results, so the arrangement of the micellar cages, which result in different mesophases with g values close to each other, appear also to be affected by the degree of ionization of surfactant and the degree of protonation of the APS, so that the mechanism requires further investigation.

As discussed above, the mesophase transformation is accompanied by a pore size shift, especially when surfactants with two hydrophilic headgroups (e.g., glutamic acid surfactant) were used as the template (Figures 3 and 10).

(32) Acharya, P.; Lopez-Quintela, M. A.; Kunieda, H.; Oshimura, E.; Sakamoto, K. *J. Oleo Sci*. **2003**, *52*, 407−420.

Scheme 3. Illustration of the Pore Size Change with Mesophase Curvature[a]

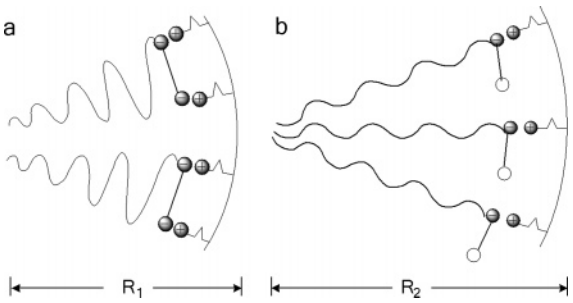

[a] Larger surface curvature with larger headgroup area (a) leads to more windings of the surfactant tails due to the van der Waals forces, which results in a smaller pore size and *d* spacings, while smaller surface curvature leads to an enlarged pore size (b).

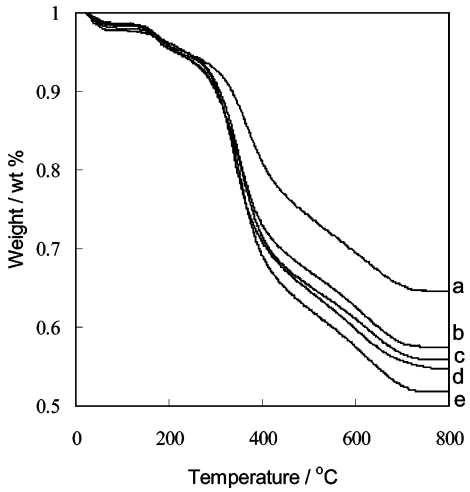

Figure 14. TG analyses of the samples GluA-AP-HCl-*x* shown in Figure 8: (a) GluA-AP-HCl-0, (b) GluA-AP-HCl-1.6, (c) GluA-AP-HCl-2.4, (d) GluA-AP-HCl-2.8, and (e) GluA-AP-HCl-3.0.

Interestingly, the mesoporous materials synthesized with the surfactant having larger effective headgroup areas often show smaller pore sizes, regardless of the type of CSDA (variably charged APS or permanently charged TMAPS). It can be imagined that the hydrophobic "tail" of the surfactant with larger effective headgroup area, rather than self-assembling loosely which is thermodynamically unfavorable, would "coil" to fill the space and thus maximize their van der Waals interactions, leading to lowering of the overall energy and the smaller pore size (Scheme 3b to a). Therefore, the driving force of the pore size change may be thermodynamic. The density of the surfactant packing in the mesopores can be confirmed by TG analyses of the samples GluA-AP-HCl-*x* as shown in Figure 14. The surfactant/SiO_2 molar ratio is increased with a decrease in the surfactant headgroup area induced by addition of HCl to the reaction system containing anionic acylglutamate surfactant. Lower surfactant packing density leads to more tightly coiled surfactant hydrocarbon tails and a smaller pore size. It can be seen that the unit cell parameter and pore size are significantly different even between the same two-dimensional hexagonal *p*6*mm* mesostructures. It can also be inferred that the surfactant/SiO_2 molar ratio in the highly ordered mesoporous material decreased in the order of $Pn\bar{3}m$ > *p*6*mm* > $Fd\bar{3}m$, $P4_2/mnm$ (GluA-TM-NaOH-*x*) with increasing surface curvatures.

It is worth noting that although the curvature of the resultant mesophases can be controlled or altered by adding different amounts of acid or base into the reaction, when different surfactants are used the specific mesophase may differ owing to the nature of the surfactants. For example, a $Pn\bar{3}m$ mesophase can be obtained as bicontinuous cubic when two-headed C_{14}GluA is used as the template, while if one-headed surfactant C_{16}ValS or C_{12}AlaA is used, the bicontinuous cubic phase is $Ia\bar{3}d$ instead. Nevertheless, control of the acidity or alkalinity of the reaction system paves a way to the mesophase control of the AMS family of mesoporous silicas.

Conclusion

Different mesostructures have been prepared by using anionic surfactant as the template and APS or TMAPS as the CSDA, by controlling the acidity or alkalinity of the reaction system. The ionization of the anionic surfactant is sensitive to the acidity or alkalinity of the solution, and surfactants with different degrees of ionization show different charge densities, which contributes to the different packing parameters *g* of the micelles and thus different silica mesostructures. It is the key factor in determining the mesophase formation. On the other hand, the positive charge density of the inorganic framework can also affect the surfactant arrangement and mesophase formation by the interactions with anionic surfactant. In addition, different mesophases can be prepared using different kinds of surfactant. Mesostructure control achieved by controlling the acidity or alkalinity of the initial reaction system is facile and simple, imparting a high degree of control to the synthesis of AMS structures and contributing to the diversity of mesophases in the AMS family.

Acknowledgment. This work was supported by the National Natural Science Foundation of China (Grants 20425102 and 20521140450), the China Ministry of Education, and the Shanghai Science Foundation (0452nm061 and 05XD14010). O.T. and Y.S. thank Swedish Science Research Council (VR) and Japan Science and Technology Agency (JST) for financial support. The authors acknowledge Prof. Paul A Wright, University of St. Andrews for critical reading.

Supporting Information Available: SEM image of the mesoporous silica GluA-TM-NaOH-2 (PDF). This material is available free of charge via the Internet at http://pubs.acs.org.

CM061107+